Composite of Hydroxyapatite-Fe₃O₄ for the Adsorption of Methylene Blue

Nur Hafizah Zainal Abidin [1]
Nonni Soraya Sambudi [,1,2]*
Norashikin Ahmad Kamal [3]

[1] *Department of Chemical Engineering, Universiti Teknologi PETRONAS, 32610 Seri Iskandar, Perak, Malaysia*

[2] *Center for Advanced Integrated Membrane System (AIMS), Universiti Teknologi PETRONAS, 32610 Seri Iskandar, Perak, Malaysia*

[3] *Department of Civil Engineering, Universiti Teknologi MARA (UiTM) Shah Alam, 40450 Selangor, Malaysia*

[*]*e-mail: soraya.sambudi@utp.edu.my*

The utilization of hydroxyapatite as an adsorbent has been extensively tested to remove the dye and heavy metal. Yet the adsorbent loss to the environment may lead to secondary pollutant issues. Consequently, the hydroxyapatite was incorporated with Fe₃O₄ amount variation to solve the secondary pollutant problem by utilizing the magnetic properties of Fe₃O₄ to recollect the adsorbent. In this work, FESEM images showed a mixture of nano-sizes rods and spherical particles corresponded to the presence of hydroxyapatite and Fe₃O₄ as a composite. The study found that hydroxyapatite- Fe₃O₄ (100 wt %) could eliminate 12.434 mg methylene blue/g adsorbent after 4 hours. The hydroxyapatite also gained improvement in its surface area from 59.8m^2/g to 75.2m^2/g when Fe₃O₄ is added. In addition, the adsorption of methylene blue fits the Freundlich isotherms and pseudo-second-order kinetic model. Furthermore, the methylene blue removal using hydroxyapatite-Fe₃O₄ composite can be kept at 80% even after 4 times experiments, showing the recyclability of hydroxyapatite-Fe₃O₄.

Keywords: Composite, Fe₃O₄, Hydroxyapatite, Methylene Blue, Recyclability

INTRODUCTION

Dye or color has been accounted for as typical contamination with high intensity, toxicity, and complex structure, which leads to difficulty in its removal (Nasar & Mashkoor 2019). Colour is a significant factor in the fabric industry, which fascinates the appearance of the textile (Kant 2012). Currently, the use of fabricated color's for texture coloring has become an enormous production industry. Furthermore, around 1.6 million liters of water are expended day by day for the typical textile industry, with the generation of 8000 kg of fabric every day (Sivasubramanian 2018). In general, water contamination of around 17% to 20% was originated from fabric coloring (Kant 2012), with roughly 7.10^5 tons of yearly utilization of the dye (Nasar and Mashkoor 2019). Due

to improper treatment of dye, its poisonous quality may harm the environment and affect all life forms. Auxochrome and chromophore in dye structure enhance the color fascination, which improves the biochemical oxygen demand (BOD) and lessens the light entrance (Nasar and Mashkoor 2019). Methylene blue is a cationic or basic dye mostly utilized for coloring purposes instead of other dyes, mainly used for wool, silk, and cotton dyeing (Gökçekuş et al. 2011).

Hydroxyapatite or $Ca_{10}(PO4)_6(OH)_2$ is a natural mineral consisting of calcium apatite that commonly exists in bone or teeth (Cui et al. 2015). It was acknowledged as the most stable calcium phosphate group under certain conditions such as pH, temperature, and fluid body composition, having common similarities with vertebrae bone (Cui et al. 2015). The calcium phosphate salt usually exists in the ratio of 1.67 of Ca/P (Eliaz and Metoki 2017). Recently, hydroxyapatite has gained attention in specific applications, especially in biomedical such as replacement of bone defect, tissue engineering systems, ear implant, and dental purpose (Eliaz et al. 2017).

In addition, non-medical applications also utilize hydroxyapatite and its derivatives, for example, a catalyst for metal oxidation, lasers material, ion conductors, and a sensor of gas (Eliaz and Metoki 2017). Furthermore, hydroxyapatite has a high impact on wastewater treatment. Hence, adsorption of heavy metal ions such as Pb^{2+} (Saber-Samandari et al. 2014), Ni^{2+} (Nguyen and Pho, 2014), Cu^{2+} (Dogan et al. 2018), Cd^{2+} (Hokkanen et al. 2018), and Zn^{2+} (Wang et al. 2018) shown that the use of hydroxyapatite as adsorbent is the best option.

Apart from that, high surface area and the existence of certain functional groups such as $-OH$ and $-HPO_4$ make hydroxyapatite to be utilized for removal of cationic dye (Janusz and Skwarek 2018). For instance, the removal of calmagite (azo dye) (Reddy et al. 2007), red dye 46 (Graba et al. 2015), methylene blue (Kyzas et al. 2015), direct yellow 27 (Mahmud et al. 2012), reactive blue 19 (Ngiyen et al. 2014), and malachite green (Hosseinzadeh and Ramin 2018) were successfully performed by using hydroxyapatite as the adsorbent. In adsorption, several techniques were implemented to improve an adsorbent's capability, such as modification of their chemical composition, which significantly increased the sorption capacity. A recent study on the application of composite adsorbent also showed an excellent performance in methylene blue adsorption.

Kaolin/sodium alginate had been proved to enhance the adsorption of methylene blue up to 78% of removal after 8 hours (Ge et al. 2019). The adsorbent's properties affected by the modifications were studied due to development of adsorbent's contact surface by improving its porosity and removal capability. Moreover, the modification was usually aimed at adding the active functional groups on the adsorbent's surface, which playing an important role for binding contaminants. Hence, in this particular study, the magnetic properties will be added to the hydroxyapatite by using Iron (III) oxide solution (Fe_3O_4) to improve the adsorption efficiency and magnetic characteristic, which will introduce the

reusability component of the material.

The hydroxyapatite-Fe$_3$O$_4$ was utilized to prevent adsorbent loss to the environment, which may lead to the further problem due to the natural properties of pure hydroxyapatite in which they are well-dispersed and highly stable in aqueous solution. Hence, nano-hydroxyapatite is hard to be isolated from aqueous solutions after usage (Tan et al. 2019). It will also lead to the possible deposition of adsorbent in the aqueous solution, causing additional water contamination. Therefore, a composite can be an alternative to address the consequence of the utilization of pure hydroxyapatite. The recollection of hydroxyapatite can be easily implemented due to the existing magnetic properties of Fe$_3$O$_4$. Despite several studies carried out on surface modification of Fe$_3$O$_4$ nanoparticles for adsorption of heavy metals and dyes, it has not been documented for the study of hydroxyapatite combined with Fe$_3$O$_4$ as composite for the removal of dyes from aqueous solutions.

The incorporation of hydroxyapatite-Fe$_3$O$_4$ was implemented using wet precipitation as this particular method has been used in producing hydroxyapatite with a larger surface area of nano-sized particles (Ramesh et al. 2015). The wet precipitation method has gained attention compared to others, such as the so-gel, due to its ability to produce higher surface area and crystalline size particles (Ramesh et al. 2015). This simple technique involves various processes such as nucleation, aggregation, agglomeration, and particle growth (Yelten-Yilmaz and Yilmaz 2018). The variation of Fe$_3$O$_4$ content shows that

surface area could be enhanced in this study. Thus, it favors more adsorption of methylene blue.

Hence, this study aims to characterize the hydroxyapatite before and after the addition of Fe$_3$O$_4$. In addition, the effect of hydroxyapatite-Fe$_3$O$_4$ on the adsorption of removal blue was also analyzed throughout this study involving the effect of contact time and initial concentration of methylene blue. The kinetics and isotherm of methylene blue removal were also investigated. The recyclability hydroxylapatite-Fe$_3$O$_4$ composite was tested and proved to be maintained at 80% removal of methylene blue, even though after four times of repetition.

MATERIALS AND METHODS
Materials

Methylene blue was purchased from Bendosen (Malaysia), while Calcium nitrate (Ca(NO$_3$)$_2$), diammonium hydrogen phosphate ((NH$_4$)$_2$PO$_4$), iron oxide (Fe$_3$O$_4$) with the mean particle size of 16.75 nm, and sodium hydroxide (NaOH) were purchased from Sigma Aldrich (USA). Hydrochloric acid (HCl) 37% was purchased from Merck (USA). All chemicals were used as received without further purification.

Synthesis of Hydroxyapatite and Hydroxyapatite-Fe$_3$O$_4$

Hydroxyapatite was acquired from the precipitation of 0.025 mol calcium nitrate mixed in 50 ml of hydrochloric acid and 0.015 mol of diammonium hydrogen phosphate mixed in 500 ml of sodium hydroxide solution. It is to give the proportion of 1.67 of Ca/P. Calcium nitrate solution was mixed at room temperature,

then continued by adding diammonium hydrogen phosphate solution by drops. The mixture was then matured for 24 hours. The precipitate acquired was filtered and washed with distilled water multiple times, followed by centrifugation to gather the precipitate. The precipitate was then dried overnight in the oven at 100°C.

The incorporation of hydroxyapatite-Fe_3O_4 was performed by following a similar synthesis method of hydroxyapatite, by adding 25 wt%, 50 wt%, and 100 wt% of Fe_3O_4 (as for the measure of pure hydroxyapatite) in calcium nitrate solution (0.025 mol in 50 ml of hydrochloric acid), and followed by adding diammonium hydrogen phosphate solution (0.015 mol in 500 ml of sodium hydroxide) by drops. The mixture was then matured, filtered, washed, and dried. The adsorbent samples that were utilized for the rest of the experiments are hydroxyapatite (HAp), Fe_3O_4, HAp-Fe_3O_4-25 (25 wt% of Fe_3O_4), HAp-Fe_3O_4-50 (50 wt% of Fe_3O_4), and HAp-Fe_3O_4-100 (100 wt% of Fe_3O_4).

Effect of Contact Time on Methylene Blue Removal

In the contact time experiment, the methylene removal was observed at an interval of 10 minutes, 30 minutes, 1 hour, 2 hours, 3 hours, 4 hours, and 5 hours by using UV Vis spectrophotometer (Shimadzu UV-1800, Japan) for the absorbance at the wavelength of 665 nm. 100 ml methylene blue solution with the initial concentration of 40 ppm was mixed with 0.5 gram of adsorbent at a speed of 200 rpm. The best adsorbent will be used for the subsequent experiment. The percentage removal of methylene blue can

be calculated as in Eq. (1):

$$\% \text{ removal} = \frac{C_0 - C_t}{C_0} \times 100\% \qquad (1)$$

Where C_0 is the initial concentration and C_t is the concentration at a different time interval.

Effect of Initial Concentration of Methylene Blue

100 ml methylene blue solution with four different initial concentrations of methylene blue, namely 40 ppm, 60 ppm, 80 ppm, and 100 ppm were prepared. Each solution was mixed with 0.5 gram of HAp-Fe_3O_4-100 as the best adsorbent, then stirred at 200 rpm. The performance in methylene blue removal was evaluated using UV Vis spectrophotometer for the absorbance at the wavelength of 665 nm after a contact time of 4 hours.

Recyclability of Hydroxyapatite-Fe_3O_4

The ability of HAp-Fe_3O_4-100 to be recycled was tested by using 100 ml solution with 40 ppm of the initial concentration of methylene blue and contact time of 4 hours. The removal of methylene blue was tested using UV Vis spectrophotometer for the absorbance at the wavelength of 665 nm. A magnet was used to collect the adsorbent and washed thrice with DI water before reused. The experiment was repeated four times.

Analysis

The surface morphology of hydroxyapatite, Fe_3O_4, and HAp-Fe_3O_4 samples was analyzed using a field emission scanning electron microscope (FE-SEM) (Ultra 55 Carl Zeiss, Germany). Fourier-transform Infrared Spectroscopy

(FT-IR) analysis (Perkin Elmar Spectrum One, USA) was conducted to deermine the functional groups present in the photocatalyst recorded at the 4000 to 500 cm^{-1} regions. The crystallinity and phase of samples were characterized using X-ray diffractometer (XRD) spectroscopy using X'Pert3 Powder & Empyrean PANalytical with Cu Kα irradiation (λ=1.54), from 10° to 70° of diffraction angles (2θ), step size of 0.01°/step, and exposure time of 1s/step. The surface area and pore size of samples were analyzed using N$_2$ physisorption analysis. Simulataneously, the dispersive energy X-ray (EDX) analysis was also done by Zeiss Supra 55 VPThe samples were degassed at 200°C followed by N$_2$ adsorption-desorption isotherms measure-ments at -196°C (Micromeritics ASAP 2020, USA).

RESULTS AND DISCUSSION

Characterization of Adsorbent

Figure 1 shows the presence of certain significant functional groups in hydroxyapatite and hydroxyapatite- Fe$_3$O$_4$. The overlapping peaks related to hydroxyapatite and iron oxide can be seen in the spectra at around 1400 cm^{-1}. The characteristics band corresponds to PO$_4^{3-}$ can be observed at around 446 cm^{-1} to 1047 cm^{-1}, which belong to hydroxyapatite (Graba et al. 2015, Gheisari et al. 2015). The absorption bands at 567 cm^{-1} and 570 cm^{-1} correspond to the $n4$ bending mode of (PO$_4^{3-}$) group, while $n3$ vibrations of (PO$_4^{3-}$) can be observed at 872–1047 cm^{-1} (Youness et al. 2018, Sambudi et al. 2016). In addition, the $v3$ vibrations of PO$_4^{3-}$ groups can be seen at 1047 and 1098 cm^{-1} (Graba et al. 2015,

Youness et al. 2018 and Sambudi et al. 2016). The functional groups of hydroxyapatite functional are represented in the range of 1080–1047 cm^{-1} that can be merged with the functional group of Fe–O (Panwar et al. 2018, Nalbandian et al. 2016) while the CO$_3^2$ intensive peaks can be found at 1400 cm^{-1} and 1636 cm^{-1} (Gheisari et al. 2015).
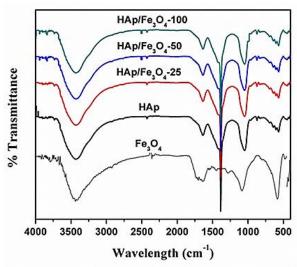

Fig. 1: FTIR spectra of adsorbents

Figure 2 shows XRD spectra of the adsorbents where diffraction angles of 25.9°, 32.07°, 33°, and 34.2° correspond to the peaks of hydroxyapatite which attributed to the planes (002), (211), (300), and (202), respectively (Kim et al. 2019). On the other hand, diffraction angles of 23.94°, 30.22°, 35.7°, 43.25°, 54°, 57.3°, and 63° indicates the appearance of iron oxide in the composite, which are attributed to (012) of Fe (Han et al. 2014), (220), (311), (440), (422), (511), and (440), respectively, which belong to Fe$_3$O$_4$ (Han et al. 2014). More peaks correspond to iron oxide in HAp-Fe$_3$O$_4$-100 than other composites, assuring a higher amount of iron oxide.
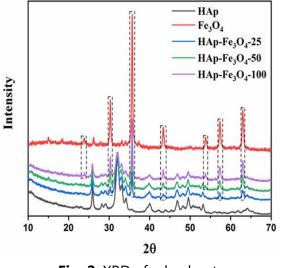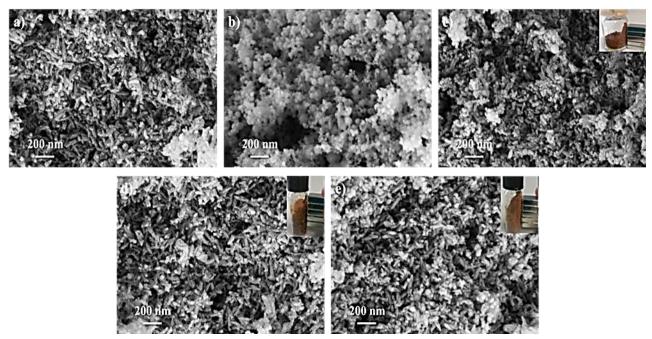
Fig. 2: XRD of adsorbents

Figure 3a shows the morphology of the hydroxyapatite, indicated by the agglomeration of nano-size rods. A previous study by Kim et al. (2019) also shows a similar observation of hydroxylapatite morphology synthesized using the wet precipitation method. On the other hand, spherical particles indicate the presence of iron oxide as shown in Figure 3b, while hydroxyapatite-Fe_3O_4 shows a clear mixture of nano-sizes rods and spherical particles correspond to the presence of both substances as a composite (Figure 3c – 3e). Magnetic attraction and van der Waals force among iron oxide were responsible for forming the agglomerates (Yusoff et al. 2017). On the other hand, the EDX result in Table 1 shows that Fe composition increases when a higher Fe_3O_4 was added into the composite. HAp- Fe_3O_4-25, HAp-Fe_3O_4-50, and HAp- Fe_3O_4-100 samples show Fe percentage of 1.35%, 6.11%, and 7.55%, respectively.

The specific surface area of materials can be analyzed through surface area and pore size analysis using nitrogen's multilayer adsorption to relative pressure. The total specific area is expressed in m^2/g. Table 2 shows the surface area and pore analysis of the adsorbents, while isotherms can be seen in Figure 4. The presence of iron oxide impacts the increment of the surface area of the hydroxyapatite composite. Surface area can be improved up to 1.3 times while pore volume up to 1.17 times when iron oxide is added. However, Figure 4c and Table 2 show that the surface area tends to decline upon the addition of the iron oxide due to their particles' aggregation (Figure 3).

Hence, this condition leads to a lower surface area (Yusoff et al. 2017, Phasuk et al. 2018). Previous studies on hydroxyapatite also exhibit high surface area, leading to a promising performance in the adsorption process (Du et al. 2018, Alqadami et al. 2018). Nanomagnetite (Fe_3O_4) particles possess promising chemical stability, low toxicity, and excellent biocompatibility to form a composite to further enhance the nanoparticles' stability and improve the number of active sites for excellent adsorption capacity (Nyankson et al. 2019). Figure 4 indicates type IV adsorption isotherms in which the adsorbents show mesoporous characteristics. The size range of 2 nm to 50 nm also indicates that the composite is mesoporous, as shown in Table 2.

Fig. 3: FESEM morphology of a) hydroxyapatite, b) Fe$_3$O$_4$, c) HAp-Fe$_3$O$_4$-25, d) HAp-Fe$_3$O$_4$-50, and e) HAp-Fe$_3$O$_4$-100.
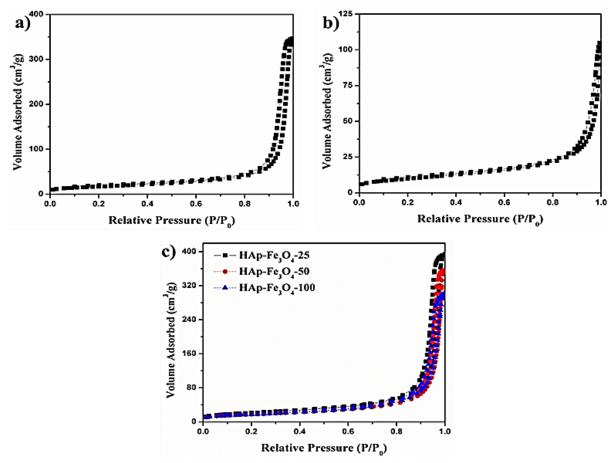

Fig. 4: N$_2$ adsorption-desorption isotherms of a) hydroxyapatite, b) Fe$_3$O$_4$, and c) HAp-Fe$_3$O$_4$

Table 1. EDX result showing elemental composition

Sample	Element (At %)		
	Ca	P	Fe
HAp	21.81	13.06	-
HAp-Fe$_3$O$_4$-25	22.69	13.59	1.35
HAp-Fe$_3$O$_4$-50	25.67	15.37	6.11
HAp-Fe$_3$O$_4$-100	30.88	18.49	7.55

Table 2. Surface area and porosity data for all adsorbents

Adsorbent	Surface Area (m^2/g)	Pore Volume (cm^3/g)	Pore Size (nm)
Fe$_3$O$_4$	35.04	0.15	16.75
Hydroxyapatite	59.8	0.52	34.9
HAp-Fe$_3$O$_4$-25	75.2	0.61	32.45
HAp-Fe$_3$O$_4$-50	62.32	0.51	33.05
HAp-Fe$_3$O$_4$-100	62.27	0.46	29.29

Methylene Blue Adsorption

The effect of contact time in methylene blue removal is shown in Figure 5a, indicating that the percentage removal increased upon longer contact time as more adsorption took place. At the beginning of the experiment, the adsorption of methylene blue on the hydroxyapatite-Fe$_3$O$_4$ was faster due to the strong electrostatic force of attraction between adsorbents and dye molecules. However, it started to become slower upon increasing the time towards the end of the experiment. At around 150- 200 minutes of contact time, there is an increment in the percentage of methylene blue removal due to the adsorbents' utilization. It happens because physical adsorption is not the only mechanism in the adsorption of methylene blue, but also involved chemical adsorption, which enhanced the adsorption capacity for methylene blue removal (Anuar et al. 2019).

It was also assumed that the dye molecules could still occupy the readily active sites of the adsorbents at this period. In general, the dye molecules need first to experience the limit layer impact, then adsorb from the surface before diffuse into the adsorbent's porous structure. The percentage removal was higher in longer contact time and eventually reached constant value as it achieved equilibrium. The saturation of the adsorption site indicating, that there are lacking vacant sites, caused the amount of methylene blue adsorbed to have remained at the same value (Aljeboree et al. 2017). In general, the methylene blue removal rate changes upon an increasing time can be related to the initially vacant sites available on the adsorbents and there is a high solute concentration gradient value (Aljeboree et al. 2017).
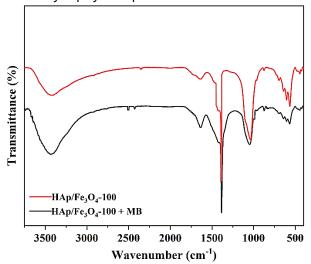
HAp-Fe$_3$O$_4$-100 was selected as the best adsorbent among others as it was able to remove up to 90% of methylene blue after four hours. In addition, the result confirmed that increasing content of iron oxide in the composite exhibits higher methylene blue removal due to the stronger force of attraction in iron oxide particles that assisted methylene blue adsorption (Phasuk et al. 2018). The higher amount of iron oxide also indicated higher magnetic particles per unit volume that enhances the affinity towards the methylene blue. The metal oxide has been

found to facilitate excellent performance in adsorption due to dipole-ion interactions of oxygen groups on metal oxide surfaces and positively charged methylene blue (Phasuk et al. 2018).

Fig. 5: a) Effect of contact time on methylene blue removal by using all adsorbents and b) effect of initial concentration on methylene blue removal by using HAp-Fe₃O₄-100

The subsequent experiment used initial concentrations of methylene blue of 40 ppm, 60 ppm, 80 ppm, and 100 ppm. Figure 5b shows the percentage removal of methylene blue with respect to dye initial concentration. HAp-Fe₃O₄-100 was the best

adsorbent compared to others, hence it was utilized in investigating the effect of initial dye concentration towards the methylene blue removal. The result shows that a higher dye initial concentration gives lower methylene blue percentage removal after a contact time of four hours. It is because the vacant site of the adsorbent was assumed to be the same at the beginning. Hence increasing initial concentration leads to the limited site for adsorption. On the other hand, the FTIR result in Figure 6 shows the functional groups before and after the methylene blue adsorption. The spectra show that no additional peak is observed after adsorption, indicating that the adsorption is mostly a physical process.

Fig. 6: FTIR spectra before and after the adsorption

Adsorption Kinetics

Pseudo-second order kinetic model was found to be well fitted in the adsorption study ,as shown in Eq. (2):

$$\frac{t}{q_t} = \frac{1}{k_2 q_e{}^2} + \frac{1}{q_e}t \qquad (2)$$

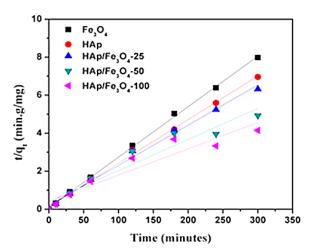Where t/q_t was plotted against time, k_2 is

pseudo-second-order rate constants of adsorption, q_e and q_t are the amount of methylene blue adsorbed (mg/g) at equilibrium and time, t respectively, and time, t denotes the adsorption time (minute). Figure 7 shows a linear plot of t/q_t vs. t. It indicates that chemisorption's mechanism was also responsible for the kinetic process (Li et al. 2018). The kinetic process for methylene blue adsorption by adsorbents excellently followed the characteristics of pseudo-second-order model's with R^2 of 0.999, 0.997, 0.993, 0.933, and 0.897 for Fe_3O_4, HAp, HAp-Fe_3O_4-25, HAp-Fe_3O_4-50, and HAp-Fe_3O_4-100, respectively.
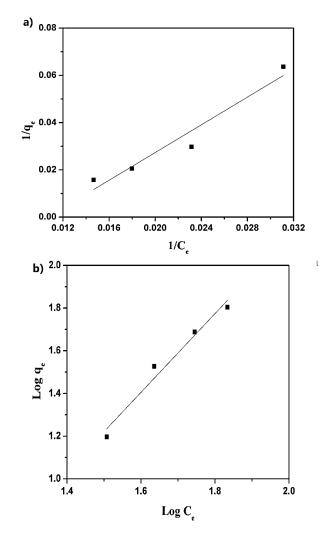
Adsorption Isotherms

Figures 8a and 8b show Langmuir and Freundlich isotherms, respectively. The analysis of isotherms shows that the adsorption of methylene blue onto the hydroxyapatite with 100 wt% Fe_3O_4 fits well the Freundlich isotherm with R^2 of 0.96. Freundlich isotherm model explains that adsorption involves heterogeneous adsorption with different layers of adsorption sites (Phasuk et al. 2018). The linearized isotherm equation that corresponds to the adsorption on the heterogeneous surface is given by Eq. (3) (Li et al. 2018):

$$\ln q_e = K_F + \frac{1}{n}(\ln C_e) \qquad (3)$$

Where q_e is the quantity of solute adsorbed at equilibrium (mg/g), K_F is the Freundlich constant related to adsorption capacity, C_e is the concentration of adsorbate at equilibrium (mg/L), and n is the Freundlich constant related to adsorption intensity of the adsorbent. From the correlation, the value of 1/n is 1.84 and K_F is 0.21.
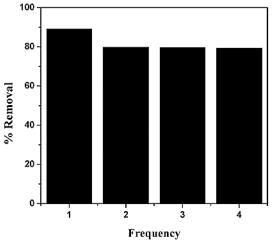

Fig. 7: Pseudo-second-order kinetic model fitting

Fig. 8: a) Langmuir and b) Freundlich isotherms fitting

Recyclability of Hydroxyapatite- Fe$_3$O$_4$

Figure 9 shows that HAp-Fe$_3$O$_4$-100 can be reused, indicating its recyclability. Furthermore, the adsorbent still gives promising results in removing methylene blue, which is around 80% during the recycling process. The percentage removal of methylene blue decrease from 89.07% to 79.87% in the second recycling process but maintained at 80% after four times of using the same adsorbent. It can be seen that the second recycling process shows a significant drop compared to the first cycle. It happens because most of the adsorbent's available active sites were completely utilized in the adsorption of methylene blue. However, the adsorbent can still be used in four cycles. Hence, this proves that HAp-Fe$_3$O$_4$-100 can be effectively utilized in removing methylene blue from the solution.

Fig. 9: Recyclability of HAp-Fe$_3$O$_4$-100

CONCLUSIONS

It is reported that hydroxyapatite-Fe$_3$O$_4$ was synthesized by wet precipitation, and its performance in methylene blue adsorption was investigated. Certain parameters such as contact time, iron oxide concentration, and initial dye concentration were studied to prove their effects on methylene blue removal. The percentage of removal was found to increase in longer contact time until it reaches equilibrium. In addition, 90% of 40 ppm methylene blue was successfully removed by using 100 wt% of iron oxide. The adsorption process also fits well pseudo-second-order kinetic model as well as Freundlich isotherm with R^2 = 0.96. Lastly, the best adsorbent recyclability, which is HAp-Fe$_3$O$_4$-100, was proven to be four times of experiment runs with methylene blue removal maintained at 80%.

REFERENCES

1. Aljeboree, A. M., Alshirifi, A. N., & Alkaim, A. F. (2017). "Kinetics and equilibrium study for the adsorption of textile dyes on coconut shell activated carbon," *Arabian J. Chem.,* S3381-S3393

2. Alqadami, A.A., Khan, M.A., M. Otero, Siddiqui, M.R., Jeon, B-H., and Batoo, K.M., (2018). "A magnetic nanocomposite produced from camel bones for an efficient adsorption of toxic metals from water," *J. Cleaner Prod., 178*, 293-304.

3. Anuar, F. I., Hadibarata, T., Muryanto, Yuniarto, A., Priyandoko, D., & Sari, A. A. (2019). "Innovative chemically modified biosorbent for removal of Procion Red,"

International Journal of Technology, *10*(4), 776–786.

4. Basirun, W. J., Nasiri-Tabrizi, B., & Baradaran, S. (2018). "Overview of Hydroxyapatite–Graphene Nanoplatelets Composite as Bone Graft Substitute: Mechanical Behavior and In-vitro Biofunctionality," *Crit. Rev. Solid State and Mater. Sci., 43*(3), 177-212.

5. Cui, L., Wang, Y., Hu, L., Gao, L., Du, B., & Wei, Q. (2015). "Mechanism of Pb(ii) and methylene blue adsorption onto magnetic carbonate hydroxyapatite/graphene oxide," *RSC Advances, 5*(13), 9759-9770.

6. Dogan, O., Bodur, B., & Inan, G. (2018). "Kinetic and thermodynamic studies of Cu(II) adsorption onto calcium phosphate," *Desalin. Water Treat., 111*, 322-328.

7. Du, K., Liu, X., Li, S., Qiao, L., & Ai, H. (2018). "Synthesis of Cu2+ Chelated Cellulose/Magnetic Hydroxyapatite Particles Hybrid Beads and Their Potential for High Specific Adsorption of Histidine-Rich Proteins," *ACS Sustainable Chem. Eng., 6*(9), 11578-11586.

8. Eliaz, N., & Metoki, N. (2017). "Calcium Phosphate Bioceramics: A Review of Their History, Structure, Properties, Coating Technologies and Biomedical Applications," *Materials (Basel, Switzerland), 10*(4), 334.

9. Ge, I. T. K., Nugraha, M. W., Ahmad Kamal, N., & Sambudi, N. S. (2019). "Composite of kaolin/sodium alginate (SA) beads for methylene blue adsorption," *ASEAN Journal of Chemical Engineering*, *19*(2), 100–109.

10. Gheisari, H., Karamian, E., & Abdellahi, M. (2015). "A novel hydroxyapatite – Hardystonite nanocomposite ceramic," *Ceram. Int., 41*(4), 5967-5975.

11. Gökçekuş, H., Umut, T., & LaMoreaux, J. W. (2011). *Survival and sustainability: concerns in the 21st century*: Springer-Verlag Berlin Heidelberg.

12. Graba, Z., Hamoudi, S., Bekka, D., Bezzi, N., & Boukherroub, R. (2015). "Influence of adsorption parameters of basic red dye 46 by the rough and treated Algerian natural phosphates," *J. Ind. Eng. Chem.", 25*, 229-238.

13. Guesmi, Y., Agougui, H., Lafi, R., Jabli, M., & Hafiane, A. (2018). "Synthesis of hydroxyapatite-sodium alginate via a co-precipitation technique for efficient adsorption of Methylene Blue dye," *J. Mol. Liq., 249*, 912-920.

14. Han, R., Li, W., Pan, W., Zhu, M., Zhou, D., & Li, F.-s. (2014). "1D Magnetic Materials of Fe3O4 and Fe with High Performance of Microwave Absorption Fabricated by Electrospinning Method," *Scientific Reports, 4*, 7493.

15. S, Hokkanen, A. Bhatnagar, V. Srivastava, V. Suorsa, and M. Sillanpää, (2018) "Removal of Cd2+, Ni2+ and PO43− from aqueous solution by hydroxyapatite-bentonite clay-nano-cellulose composite," *Int. J. Biol. Macromol.*, (118), 903-912.

16. Hosseinzadeh, H., & Ramin, S. (2018). "Fabrication of starch-graft-poly(acrylamide)/graphene oxide/hydroxylapatite nanocomposite hydrogel adsorbent for removal of malachite green dye from aqueous solution," *Int. J. Biol. Macromol., 106*, 101-115.

17. Janusz, W., & Skwarek, E. (2018). "Effect of Co(II) ions adsorption in the

hydroxyapatite/aqueous NaClO$_4$ solution system on particles electrokinetics." *Physicochem. Probl. Miner. Process., 54*, 31-39.

18. Kant, R. (2012). "Textile dyeing industry an environmental hazard," *Natural Science, Vol.04 No.01*, 5.

19. Kim, J., Sambudi, N. S., & Cho, K. (2019). "Removal of Sr2+ using high-surface-area hydroxyapatite synthesized by non-additive in-situ precipitation," *J. Environ. Manage., 231*, 788-794.

20. Li, L., Iqbal, J., Zhu, Y., Zhang, P., Chen, W., Bhatnagar, A., et al., "Chitosan/Ag-hydroxyapatite nanocomposite beads as a potential adsorbent for the efficient removal of toxic aquatic pollutants, "*Int. J. Biol. Macromol.*, (120), 1752-1759, 2018/12/01/ 2018.

21. Mahmud, K., Azharul Islam, M., Mitsionis, A., Albanis, T., & Vaimakis, T. (2012). "Adsorption of direct yellow 27 from water by poorly crystalline hydroxyapatite prepared via precipitation method," *Desalin. Water Treat., 41*(1-3), 170-178.

22. Nalbandian, L., Patrikiadou, E., Zaspalis, V., Patrikidou, A., Hatzidaki, E., & N. Papandreou, C. (2016). "Magnetic Nanoparticles in Medical Diagnostic Applications: Synthesis, Characterization, and Proteins Conjugation," *Curr. Nanosci., 12*(4), 455-468.

23. Nasar, A., & Mashkoor, F. (2019). "Application of polyaniline-based adsorbents for dye removal from water and wastewater review," *Environ. Sci. Pollut. Res., 26*(6), 5333-5356.

24. Nguyen, V. C., & Pho, Q. H. (2014). "Preparation of Chitosan Coated Magnetic Hydroxyapatite Nano-particles and Application for Adsorption of Reactive Blue 19 and Ni2+ Ions," *Sci. World J.*

25. Nyankson, E., Adjasoo, J., Efavi, J. K., Amedalor, R., Yaya, A., Manu, G. P., ... Amartey, N. A. (2019). "Characterization and evaluation of zeolite A/Fe3O4 nanocomposite as a potential adsorbent for removal of organic molecules from wastewater," *J. Chem*.

26. Panwar, V., Kumar, P., Bansal, Ray, S.S., and Jain, S.L., (2015) "PEGylated magnetic nanoparticles (PEG@Fe3O4) as cost effective alternative for oxidative cyanation of tertiary amines via CH activation," *Appl. Catal., A*, (498), 25-31, 2015/06/05/ 2015.

27. Phasuk, A., Srisantitham, S., Tuntulani, T., & Anutrasakda, W. (2018). "Facile synthesis of magnetic hydroxyapatite-supported nickel oxide nanocomposite and its dye adsorption characteristics," *Adsorption, 24*(2), 157-167.

28. Ramesh,S, A. N. Natasha, C. Y. Tan, L. T. Bang, A. Niakan, J. Purbolaksono, et al., (2015) "Characteristics and properties of hydoxyapatite derived by sol–gel and wet chemical precipitation methods," *Ceram. Int.*, (41), 10434-10441.

29. Reddy, M. P., Venugopal, A., & Subrahmanyam, M. (2007). "Hydroxyapatite photocatalytic degradation of calmagite (an azo dye) in aqueous suspension," *Appl. Catal., B, 69*(3), 164-170.

30. Saber-Samandari, S., Saber-Samandari, S., Nezafati, N., & Yahya, K. (2014). "Efficient removal of lead (II) ions and methylene blue from aqueous solution using chitosan/Fe-hydroxyapatite

nanocomposite beads," *Journal of Environmen. Manage., 146*, 481-490.

31. Sambudi, N.S., Cho, S., and Cho, K. (2016) "Porous hollow hydroxyapatite microspheres synthesized by spray pyrolysis using a microalga template: preparation, drug delivery, and bioactivity," *RSC Advances*, (6), 43041-43048.

32. Sivasubramanian, V. (2018). *Bioprocess Engineering for a Green Environment* (1 ed.): CRC Press.

33. Tan, Y., Liu, Y., Luo, S., & Li, J. (2019). *Hydroxyapatite Applications in Environmental Monitoring and Treatment Advances in Chemical Engineering*. (September). Retrieved from www.openaccessebooks.com.

34. Wang, Y.-X. Liu, H.-H. Lu, R.-Q. Yang, and S.-M. Yang, "Competitive adsorption of Pb(II), Cu(II), and Zn(II) ions onto hydroxyapatite-biochar nanocomposite in aqueous solutions," *J. Solid State Chem.*, (261), 53-61.

35. Yelten-Yilmaz, A., & Yilmaz, S. (2018). "Wet chemical precipitation synthesis of hydroxyapatite (HA) powders," *Ceram. Int., 44*(8), 9703-9710.

36. Youness, R. A., Taha, M. A., El-Kheshen, A. A., & Ibrahim, M. (2018). "Influence of the addition of carbonated hydroxyapatite and selenium dioxide on mechanical properties and in vitro bioactivity of borosilicate inert glass," *Ceram. Int., 44*(17), 20677-20685.

37. Yusoff, A. H. M., Salimi, M. N., & Jamlos, M. F. (2017). "Synthesis and characterization of biocompatible Fe3O4 nanoparticles at different pH," *AIP Conference Proceedings, 1835*(1), 020010.